Particle Trajectory Tracing and Computational Electromagnetics for Accelerator and Related Technologies

Carlos Alexandre F. Jorge, Reinaldo J. Jospin, José A. D. Furlanetto
Instituto de Engenharia Nuclear, CNEN, Via Cinco, s/n, 21.945-970, Rio de Janeiro, RJ
{calexandre, rj.jospin, furla}@ien.gov.br

***Abstract*— The main objective of this R&D work is to simulate particle beam optics in CV-28 Cyclotron of Instituto de Engenharia Nuclear – IEN/CNEN, as a support for improvements or optimization of this particle accelerator. Besides 2D magnetostatic field computation results, the authors present an alternative method for charged particle trajectories computation in electrostatic or magnetostatic fields. This task is approached by analytical computation of trajectories, by parts, considering constant fields within each finite element. This method has some advantages over numerical integration ones: numerical miscomputation of trajectories is avoided; stability problem is also avoided, for the magnetostatic field case. Some examples are presented, including positive ion extraction from cyclotrons with strip-foil. This latter technique is an interesting alternative for upgrading positive ion cyclotrons, such as CV-28 Cyclotron. The particle trajectory computation method presented in this work is of interest not only for cyclotrons, but for accelerator and related technology, in general.**

***Index Terms*—** Computational electromagnetics, cyclotron, particle trajectory computation, stripping extraction of positive ions.

I. INTRODUCTION

CV-28 Cyclotron [1] particle accelerator of IEN/CNEN, is under operation since 1974. Originally designed as a multi-particle, variable energy cyclotron, it is currently dedicated to accelerate only 24 MeV protons, for medical radioisotopes production. This accelerator could have, thus, its design optimized for this particular application.

One possible improvement could be the use of strip-foils for beam extraction, instead of electrostatic deflection system, the latter currently used in CV-28 Cyclotron. The use of strip-foils would minimize beam losses, and also operational and maintenance problems. The electrostatic deflector is one of the most activated parts in a cyclotron of this type, what causes higher radiation doses for workers during maintenance. Also, in this Cyclotron, extraction efficiency achieved with electrostatic deflection is approximately 70 %, while the use of strip-foils can lead to extraction efficiencies near 100 % [2].

Such an improvement can be strongly supported by particle beam optics analysis. Then, an R&D has begun in IEN, for computational electromagnetics and particle trajectory computation [3], [4],

Brazilian Microwave and Optoelectronics Society-SBMO *Received 10 Aug., 2006; revised 16 Feb., 2007; accepted 27 April 2007*
ISSN 1516-7399

based on a finite element package formerly developed.

Previous results have been reported [5]. New results include 2D fields computation from vector potentials, and particle trajectory computation in electrostatic or magnetostatic fields [4]. The last task is performed for single non-relativistic particle, space charge effects are not considered for beam simulation in the current stage.

Some authors [6]-[8], report particle trajectory computation in electromagnetic fields by numerical integration methods. In the present work, though, as linear finite elements are used, trajectory computation can be performed analytically, on an element-by-element basis, taking into account the constant (electrostatic or magnetostatic) fields within each finite element. This approach is an alternative to the use of numerical integration methods [6], [7].

This method is similar to the one reported in [9]. Those authors, though, have only briefly described it in words, giving no details about formulations. Thus, as long as no information was available, all the formulations had to be derived, as well as the strategies adopted for particle advance within the mesh. The authors propose, in the present work, detailed formulations for this alternative method.

Some of its characteristics are compared to numerical integration's ones:

1- Trajectory is computed analytically within each finite element, then approximation deviations due to numerical integration are avoided; it requires, though, constant fields within each element.

2- Stability problem in trajectory computation can be avoided, by solving system of equations directly for coordinates; in numerical integration methods, care must be taken in the time step choice, in the magnetostatic field case, for stability [7], [8].

3- No matrix inversion is required, as it does in numerical integration methods [7], for the magnetic field case.

4- At each step, trajectory interception with the next finite element's frontier must be identified and computed correctly, what is not required in numerical integration methods.

Some examples illustrate the method. Among them, simulations are performed for extraction of positive ions from cyclotrons with strip-foils. This technique is a very interesting alternative for the use of electrostatic deflection systems, also avoiding all the technological difficulties related to negative ion cyclotron design or upgrade.

II. 2D FIELD FORMULATIONS

A. Differential equation

The formulation for magnetostatics is based on the magnetic vector potential, as shown in (1).

$$\nabla \times \nu \nabla \times \mathbf{A} = \mathbf{J} \tag{1}$$

where:

- **A** and **J** are the vector potential and the applied current density source, respectively,
- ν is the magnetic reluctivity, which in this work is considered to be uniform for the iron regions.

Brazilian Microwave and Optoelectronics Society-SBMO Received 10 Aug., 2006; revised 16 Feb., 2007; accepted 27 April 2007
ISSN 1516-7399

In a 2D domain Ω, (1) reduces to the Poisson equation in (2).

$$\nabla \cdot \nu \nabla A = -J \tag{2}$$

where:

- A and J are components of **A** and **J**, respectively, in the normal out of plane direction.

B. Weak formulation

From Galerkin weighted residuals approach, it follows the weak integral formulation (3) over the domain Ω, with boundary Γ.

$$\int_{\Omega} \nabla w \cdot \nu \nabla \hat{A} d\Omega - \oint_{\Gamma} w \nu \nabla \hat{A} \cdot \mathbf{n} \, d\Gamma = \int_{\Omega} w J d\Omega \tag{3}$$

where:

- $\hat{A}$ is the estimate for the potential A,
- w is the weighting function,
- **n** is the outward unity vector normal to the boundary Γ.

C. Finite element discretization

First-order triangular finite elements were used [10]. Discrete formulation for the 2D Cartesian referential system, results [11] in (4).

$$\sum_{NE} \left[\nu_e \int_{\Omega e} \left(\frac{\partial w_e}{\partial x} \frac{\partial \hat{A}_e}{\partial x} + \frac{\partial w_e}{\partial y} \frac{\partial \hat{A}_e}{\partial y} \right) dxdy \right] = \sum_{NE} \left[\nu_e \frac{\partial \hat{A}}{\partial \mathbf{n}} \oint_{\Gamma} w_e \, d\Gamma + J_e \int_{\Omega e} w_e dxdy \right] \tag{4}$$

where:

- the subscript e denotes element,
- Ωe denotes the element subdomain,
- NE is the number of elements in the domain Ω,
- ν and J are constant within each element.

III. PARTICLE TRAJECTORY COMPUTATION

A. Element identification algorithm

For particle trajectory computation, the finite element that contains the particle, must be identified, at any moment, given particle's coordinates. A strategy for this task has been implemented, based on Lohner's algorithm [12]. The steps of this strategy are explained in the following, for 2D triangular finite element meshes.

1- Select an element, and evaluate its interpolation functions N_i, for the given Cartesian coordinates (x, y);
2- If, for all i, $N_i > 0$ and $N_i <= 1$, then the point (x, y) is located within the selected element;
3- If not, find the minimum algebraic value of N_i, and select the neighbor element that faces the opposite side of this node;
4- Evaluate again N_i, return to step 2.

Step number 3 directs the search towards the given coordinates (x, y). This algorithm, independent

Brazilian Microwave and Optoelectronics Society-SBMO Received 10 Aug., 2006; revised 16 Feb., 2007; accepted 27 April 2007
ISSN 1516-7399

of the first element selected, finds the element that contains the coordinate (x, y) faster than an exhaustive search in the entire mesh.

B. Trajectory computation

In numerical integration methods, particle's velocity is updated first, and then its coordinates. Also, as the fields may vary in a more general way within the domain, algorithms such as Leap-Frog, consider values of variables at half time steps [6], [7], so as to improve results. For the magnetic field case, though, the resulting system of equations shows interdependence between velocity components along the coordinate axes, and its solution requires matrix inversion [7]. Also, the time step must be carefully chosen, for stability in trajectory integration [7], [8].

But since in this work, the fields are constant within finite elements, there is no need to consider variables at half time steps. Acceleration's value is given for each finite element, and velocity and coordinates' initial values are the ones at the beginning frontier. Further, as the intersection between particle's trajectory and the element's frontiers has to be computed at each step, coordinates are updated first, and then velocity.

The general formulations for particle's coordinates and velocity are shown in the following. Solution is derived first for this general formulation, the particular cases for electrostatic and magnetostatic fields are shown late.

$$\mathbf{r}_i = \mathbf{r}_{i-1} + \mathbf{v}_{i-1}\Delta t + (1/2)\mathbf{a}^e \Delta t^2 \tag{5}$$

$$\mathbf{v}_i = \mathbf{v}_{i-1} + \mathbf{a}^e \Delta t \tag{6}$$

where:

- $\mathbf{r}_i$ is particle's updated coordinate, with initial value (on the initial frontier) $\mathbf{r}_{i-1}$,
- $\mathbf{v}_i$ is particle's updated vector velocity, with initial value $\mathbf{v}_{i-1}$,
- $\mathbf{a}^e$ is particle's acceleration within each element,

The equation of a frontier's support line of a generic finite element, say for frontier 12, is:

$$y = \left(\frac{y_2 - y_1}{x_2 - x_1} \right) x + \frac{x_2 y_1 - x_1 y_2}{x_2 - x_1} \tag{7}$$

where:

- (x_1, y_1) and (x_2, y_2), are Cartesian coordinates of element's nodes 1 and 2, respectively.

All calculations are shown for frontier 12. For the other frontiers, 23 and 31, cyclic permutation of indexes has to be performed, whenever needed.

Cartesian components x_i and y_i of coordinate $\mathbf{r}_i$ in (5), plus the finite element frontier's formulations in (7), form a system of three equations, with three unknowns: Δt, x_i and y_i, – by changing x and y variables in (7), for x_i and y_i, respectively.

The solution of this system of equations gives intersections between trajectory curve and the finite element's frontiers. It may be solved by two approaches:

1- System of equations solved for the time interval variable, and then coordinates computed;

Brazilian Microwave and Optoelectronics Society-SBMO *Received 10 Aug., 2006; revised 16 Feb., 2007; accepted 27 April 2007*
ISSN 1516-7399

2- System of equations solved directly for coordinates, which are the desired variables.

Each one is explained in more details in the following.

1) Trajectory computation from time interval variable:

From (5) and (7), solving for the time interval Δt results, after some algebraic manipulation:

$$\frac{1}{2}\left[(y_2-y_1)a_x^e-(x_2-x_1)a_y^e\right]\Delta t^2+\left[(y_2-y_1)v_{x\,i-1}-(x_2-x_1)v_{y\,i-1}\right]\Delta t+ \\ +(y_2-y_1)x_{i-1}-(x_2-x_1)y_{i-1}+x_2y_1-x_1y_2=0 \tag{8}$$

which is a second order equation in Δt, where:

- a_x^e and a_y^e are Cartesian components of acceleration $\mathbf{a}^e$,
- $v_{x\,i-1}$ and $v_{y\,i-1}$ are Cartesian components of initial velocity $\mathbf{v}_{i-1}$.

Thus, the time interval spent by the particle up to the frontier 12 can be solved as:

$$\Delta t_{12}=\frac{-B\pm\sqrt{\Delta}}{2A} \tag{9a}$$

where:

$$A=\frac{1}{2}\left[(y_2-y_1)a_x^e-(x_2-x_1)a_y^e\right] \tag{9b}$$

$$B=(y_2-y_1)v_{x\,i-1}-(x_2-x_1)v_{y_{i-1}} \tag{9c}$$

$$C=(y_2-y_1)x_{i-1}-(x_2-x_1)y_{i-1}+x_2y_1-x_1y_2 \tag{9d}$$

$$\Delta=B^2-4AC=\left[(y_2-y_1)v_{x\,i-1}-(x_2-x_1)v_{y_{i-1}}\right]^2 \\ -2\left[(y_2-y_1)a_x^e-(x_2-x_1)a_y^e\right]\left[(y_2-y_1)x_{i-1}-(x_2-x_1)y_{i-1}+x_2y_1-x_1y_2\right] \tag{9e}$$

Normalization is performed for parameters A, B and C, by dividing each one by A, if $A \neq 0$.

The time interval Δt may have, in general, two distinct solutions for each frontier, resulting in a total of six solutions. Let's consider the situations that may arise. Lets call Δt_a and Δt_b the two distinct possible solutions for the current frontier:

1- If $\Delta > 0$ in (9a), two situations may occur:

a) If $\Delta t_a > 0$, $\Delta t_b > 0$ and $\Delta t_a < \Delta t_b$:

The correct solution is Δt_a, which corresponds to the nearest intersection; Δt_b corresponds to a farther intersection, possibly outside the current finite element.

b) If $\Delta t_a > 0$ and $\Delta t_b < 0$:

The correct solution is Δt_a, as the negative one would correspond to a particle moving in the opposite direction, with a negative velocity.

2- If $\Delta = 0$, in (9a):

The formulation, (8), reduces to a first order equation, and has only one solution; the particle intercepts the current frontier only once: crossing it, or tangent to it.

3- If $\Delta < 0$, in (9a):

Brazilian Microwave and Optoelectronics Society-SBMO *Received 10 Aug., 2006; revised 16 Feb., 2007; accepted 27 April 2007*
ISSN 1516-7399

There is no solution; the particle does not intercept the current frontier.

4- If $A = 0$, in (9a):

In this case, (9a) can not be directly used, but (8) also reduces to a first order equation, from which Δt_{12} can be solved as:

$$\Delta t_{12} = -\frac{C}{B} \tag{9f}$$

This case corresponds also to the situations where the particle intercepts the current frontier only once: crossing it, or tangent to it.

The correct overall solution, among all six possible ones, corresponds to the lower non-zero positive solution; non-zero because a null Δt corresponds, in fact, to the initial point for the particle's trajectory computation, and not to a solution itself.

Once identified, the correct solution for Δt is then used to advance the particle up to the next frontier, updating particle's coordinates with (5), and particle's velocity with (6). This process is repeated, on an element-by-element basis.

The specific solutions for electrostatic and for magnetostatic field cases are detailed in the following:

Electrostatic field case:

Particle acceleration due to electrostatic field is:

$$\mathbf{a}^e = \frac{q}{m}\mathbf{E}^e \tag{10}$$

where:

- $\mathbf{E}^e$ is the constant electric field within the current element.

The solution is obtained by substituting Cartesian components a_x^e and a_y^e of the acceleration given by (10) in (9b) and (9e), and solving (9a).

It is important to notice that this approach can be extended to a generic 2D trajectory. Since the electrostatic field is constant within each finite element, the trajectory is computed as a parabola for each element, but the whole trajectory can be any generic curve.

Magnetostatic field case:

Let's consider a 2D circular trajectory, as shown in Fig. 1, to define a referential Cartesian coordinate system. The only magnetic field component is along the *z*-axis, as indicated. The particle moves clockwise in the *x*-*y* plane, describing a circumference with radius ρ, the Larmor radius; the increasing direction adopted for the angle θ in this referential system, though, is counterclockwise. Particle's initial parameters are also indicated: velocity $\mathbf{v}_{i-1}$, angle with horizontal θ_{i-1}, coordinates (x_{i-1}, y_{i-1}), besides charge q and mass m. The circumference center's coordinates are (x_C, y_C).

Brazilian Microwave and Optoelectronics Society-SBMO *Received 10 Aug., 2006; revised 16 Feb., 2007; accepted 27 April 2007*
ISSN 1516-7399

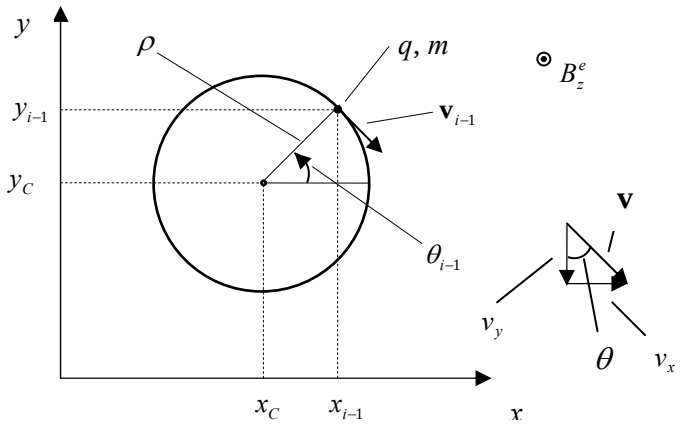

Fig. 1. Particle's circular trajectory in magnetostatic field.

Particle's acceleration due to the magnetostatic field, in 2D, is given by:

$$\mathbf{a} = \frac{q}{m}\mathbf{v} \times \mathrm{B} \quad \therefore \quad \begin{cases} a_x^e = \omega_C v_{y\,i-1} \\ a_y^e = -\omega_C v_{x\,i-1} \end{cases} \tag{11}$$

where:

- ω_C is the cyclotronic frequency, given by:

$$\omega_C = \frac{q}{m} B_z^e \tag{12}$$

and:

- B_z^e is the constant magnetic field component in the z-axis, within the current element.

The solution is obtained by substituting the acceleration components (11) in (9b) and (9e), and solving (9a).

This approach, though, when implemented, has led to miscalculations in trajectory, increasing with time advance, due to the approximation of the circular trajectory by parabolas, within each element. Thus, for the magnetostatic field case, this approach has been discarded, and the one adopted considers solution by coordinates, as explained in the following.

2) Trajectory computation directly for coordinates:

In this case, the solution could be obtained, through a general approach, using (5) and (7), but eliminating the time interval Δt, and solving the system of equations for the coordinates x_i and y_i. An alternative for the magnetic field case is to consider particle's circular trajectory within each finite element. Both approaches are explained in the following.

General formulation:

From (5) and (7), solving for the coordinates x_i and y_i, results, after some algebraic manipulation:

$$a_y^e\left(v_{x\,i-1} \pm \sqrt{v_{x\,i-1}^2 + 2a_x^e\left(x_i - x_{i-1}\right)}\right) = a_x^e\left(v_{y\,i-1} \pm \sqrt{v_{y\,i-1}^2 + 2a_y^e\left(y_i - y_{i-1}\right)}\right) \tag{13}$$

Thus, a system of two equations results from (13) and (7) – repeated here as (14) for convenience.

Received 10 Aug., 2006; revised 16 Feb., 2007; accepted 27 April 2007
ISSN 1516-7399

$$y = \left(\frac{y_2 - y_1}{x_2 - x_1} \right) x + \frac{x_2 y_1 - x_1 y_2}{x_2 - x_1} \tag{14}$$

This system of equations, though, results in an intricate formulation to be solved. Then, this approach has been discarded, and trajectory computation from time interval variable Δt, already presented in (9a) through (9f), is preferred for the electrostatic field case; for the magnetostatic one, an alternative approach is explained in the following.

Circular trajectory formulation:

The solution for the magnetostatic field case, obtained directly for coordinates, can also be approached, in 2D Cartesian coordinates, through the direct use of the circular trajectory formula (15).

$$x = x_C \pm \left[\rho^2 - (y - y_C)^2 \right]^{1/2} \tag{15}$$

where:

- ρ is the Larmor radius,
- (x_C, y_C) is the trajectory center's coordinates.

The Larmor radius is computed as:

$$\rho = \frac{|\mathbf{v}|}{\omega_C} \tag{16}$$

where:

- $|\mathbf{v}|$ is velocity's magnitude, constant within each finite element.

The trajectory center's coordinates are computed, for the current element, as:

$$\begin{cases} x_C = x_{i-1} - \rho \cos\theta_{i-1} \\ y_C = y_{i-1} - \rho \sin\theta_{i-1} \end{cases} \tag{17}$$

where:

- θ_{i-1} is the angle between $\mathbf{v}_{i-1}$ and the horizontal, in counterclockwise direction, as shown in Fig. 1.

The initial angle θ_{i-1} is computed, for the current element, as:

$$\theta_{i-1} = \tan^{-1}\left(\frac{v_{xi-1}}{-v_{yi-1}} \right) \tag{18}$$

A system of equations, resulting from (15) and (14), has to be solved for the coordinates x_i and y_i, resulting, after some algebraic manipulation, in (18):

$$\begin{aligned} &\left[(x_2 - x_1)^2 + (y_2 - y_1)^2 \right] x_i^2 + \\ &+ 2\left\{ (y_2 - y_1)\left[x_2 y_1 - x_1 y_2 - y_C (x_2 - x_1) \right] - x_C (x_2 - x_1)^2 \right\} x_i + \\ &+ \left[x_2 y_1 - x_1 y_2 - y_C (x_2 - x_1) \right]^2 + x_C^2 (x_2 - x_1)^2 - \rho^2 (x_2 - x_1)^2 = 0 \end{aligned} \tag{19}$$

which is a second order equation in x_i.

Thus, updated particle's coordinates in the next frontier can be solved as:

$$x_i = \frac{-B \pm \sqrt{\Delta}}{2A} \tag{20a}$$

where:

$$A = (x_2 - x_1)^2 + (y_2 - y_1)^2 \tag{20b}$$

$$B = 2\left\{(y_2 - y_1)\left[x_2 y_1 - x_1 y_2 - y_C (x_2 - x_1)\right] - x_C (x_2 - x_1)^2\right\} \tag{20c}$$

$$C = \left[x_2 y_1 - x_1 y_2 - y_C (x_2 - x_1)\right]^2 + x_C^2 (x_2 - x_1)^2 - \rho^2 (x_2 - x_1)^2 \tag{20d}$$

$$\begin{aligned}\Delta = B^2 - 4AC = &\left[2\left\{(y_2 - y_1)\left[x_2 y_1 - x_1 y_2 - y_C (x_2 - x_1)\right] - x_C (x_2 - x_1)^2\right\}\right]^2 \\ &- 4\left[(x_2 - x_1)^2 + (y_2 - y_1)^2\right]\left\{\left[x_2 y_1 - x_1 y_2 - y_C (x_2 - x_1)\right]^2 + \right. \\ &\left. + x_C^2 (x_2 - x_1)^2 - \rho^2 (x_2 - x_1)^2\right\}\end{aligned} \tag{20e}$$

Normalization is also performed in parameters A, B and C, if $A \neq 0$. Once the coordinate x_i is found, the correspondent coordinate y_i must be computed, with (14).

There are also, in general, two distinct solutions for each frontier, resulting in a total of six solutions. Let's consider the situations that may arise:

1- If $\Delta > 0$ in (20a):

The particle's trajectory intercepts the current frontier twice; the correct solution corresponds to the one that gives the lowest distance to the initial point (x_{i-1}, y_{i-1}).

2- If $\Delta = 0$ in (20a):

There is only one solution; the particle's trajectory is tangent to the current frontier.

3- If $\Delta < 0$ in (20a):

There is no solution; the particle's trajectory does not intercept the current frontier.

The correct overall solution corresponds to the one that gives the lowest distance to the initial point (x_{i-1}, y_{i-1}).

It is important to notice again, that this approach can be extended to a generic 2D trajectory. The trajectory is approximated, for each finite element, by circular arcs, but the whole trajectory can be anyone. Larmor radius, cyclotronic frequency and trajectory's center coordinates, must be computed for each element.

In summary:

1- The approach for time Δt variable solution is preferred for the electrostatic field case, for which it gives good results. For the magnetostatic field case, this approach should be further investigated for minimum Δt which gives good results.

2- The approach for coordinate variables (x_i, y_i) solution is preferred for the magnetostatic field case, considering circular particle trajectory by parts. For the electrostatic field case, the coordinates solution results in an intricate formulation.

IV. STRIP-FOIL EXTRACTION SYSTEMS FOR CYCLOTRONS

Extraction systems based on strip-foils – also known as charge-exchange beam extraction – was invented in 1964 [13], with first experimental results reported some years latter [13].

Some important concepts for ion extraction are reviewed in the following. The charge state Z refers to the number of charges in an ion, while the mass number A refers to the number of nucleons –

Brazilian Microwave and Optoelectronics Society-SBMO *Received 10 Aug., 2006; revised 16 Feb., 2007; accepted 27 April 2007*
ISSN 1516-7399

Proton or Neutrons – in an ion. Specific charge η, in turn, means the ratio Z/A, while the ratio of specific charge change after and before stripping extraction is given as $K = \eta_a/\eta_b$ [13], where:

- η_b is the specific charge before stripping,
- η_a is the specific charge after stripping.

From (12) and (16), Larmor radius ρ can be expressed as:

$$\rho = \frac{mv}{qB} \tag{21}$$

As variations in Z correspond directly to variations in q, when Z increases, so do q, and from (21), Larmor radius decreases.

This technique has been widely used for negative ion beam extraction [2], [13]. Negative ions loose electrons when passing through the strip-foil, becoming positive ions. The rotation direction is thus changed, and ions are directed towards cyclotron's exit.

The strip-foil technique can also be used for positive ion extraction [13], [14]. In this case, a positive ion looses electrons in the strip-foil, and its charge state Z increases, reducing its rotation radius. The positive ion, thus, performs at least one short loop, before exiting the cyclotron [13]-[15].

As cyclotron electromagnetic fields are not designed to take into account this kind of motion, beam quality may be disturbed [13], [15], thus, multiple loops should be avoided. Also, the specific charge η must increase at least by 2, so the rotation radius decreases at least by 0.5, preventing the ion to perform an additional orbit through the cyclotron, which would result in additional acceleration [15].

Light positive ions can be extracted with high efficiency, near 100 %, while extraction efficiency for heavy positive ions is poorer [13], [16], for the following reason: due to the diversity of charge states resulting after a heavy positive ion passes through a strip-foil [17], [18]; thus, only ions of one of these charge states can be extracted in a given design.

Some common examples of negative and positive ion extraction can be mentioned:

1- Both H^+ and H^- Hydrogen ions have charge state $Z = 1$, mass number $A = 1$, and consequently, specific charge $\eta = 1$. The former must be extracted by electrostatic deflection, while the latter is stripped with $K = -1$, [13], [15].

2- Both $^2H^+$ and $^2H^-$ Deuteron ions, have charge state $Z = 1$, mass number $A = 2$, and consequently, specific charge $\eta = 0.5$. The former must be extracted by electrostatic deflection, while the latter is stripped to $^2H^+$ with $K = -1$, [13], [15].

3- Molecular Hydrogen ion H_2^+ has charge state $Z = 1$, mass number $A = 2$, and consequently, specific charge $\eta = 0.5$. When stripped, it dissociates into two Protons, with $K = 2$, [13], [15].

4- He^+ has charge state $Z = 1$, mass number $A = 4$, and consequently, specific charge $\eta = 0.25$. It is stripped to He^{++}, with $K = 2$.

Brazilian Microwave and Optoelectronics Society-SBMO *Received 10 Aug., 2006; revised 16 Feb., 2007; accepted 27 April 2007*
ISSN 1516-7399

V. NUMERICAL RESULTS

A. Magnetostatic fields – vector potential

1) Bastos' example:

The first example, reported in [19], is illustrated in Fig. 2, which shows the input data for the problem. A mesh with the same characteristics as the one reported in [19], has been generated, for comparison purposes.

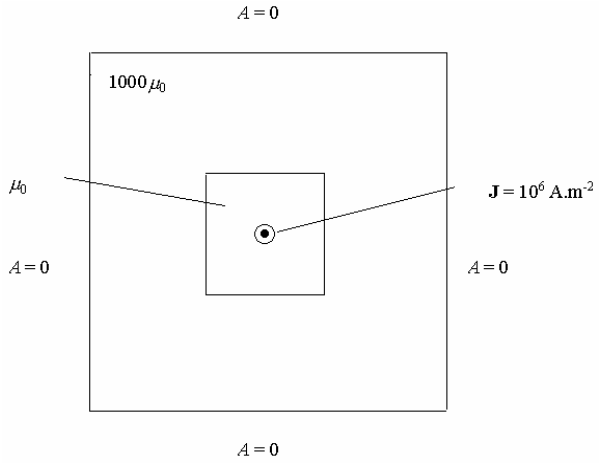

Fig. 2. Bastos' example geometry.

Results for the *z*-axis component of the magnetic vector potential *A*, for six nodes in the domain, are compared in Table I.

TABLE I. BASTOS' EXAMPLE – VECTOR POTENTIAL *A*

Node	***A*** **[Wb.m^{-1}] (×10^{-2}): Bastos' results**	***A*** **[Wb.m^{-1}] (×10^{-2}): IEN's results**
4	1.5325	1.5325
8	3.0651	3.0649
12	3.3723	3.3722
13	3.3723	3.3722
14	7.3598	7.3594
30	3.0645	3.0643

Comparison of the magnetic induction components B_x and B_y for six elements in the domain, is shown in Table II.

TABLE II. BASTOS' EXAMPLE – INDUCTION COMPONENTS *BX*, *BY*

Element	***Bx*** **[T]: Bastos' results**	***Bx*** **[T]: IEN's results**	***By*** **[T]: Bastos' results**	***By*** **[T]: IEN's results**
4	3.0726×10^{-1}	3.0726×10^{-1}	-3.9875	-3.9875
8	3.1411×10^{-3}	3.1415×10^{-3}	-4.3876×10^{-3}	-4.3872×10^{-3}
12	6.4760×10^{-3}	6.4764×10^{-3}	6.4760×10^{-3}	6.4764×10^{-3}
13	0.	0.	3.0645	3.0645
14	4.2903	4.2901	-1.5325	-1.5325
30	1.5325	1.5325	-4.2903	-4.2903

Brazilian Microwave and Optoelectronics Society-SBMO *Received 10 Aug., 2006; revised 16 Feb., 2007; accepted 27 April 2007*
ISSN 1516-7399

2) Steering magnetic device:

The second example is based on a magnetic steering device developed previously at IEN [20]. Results obtained in the present work are compared to both Meeker's FEMM [21] results and to experimental measurements.

The magnetic steering device's geometry is shown in Fig. 3a. Plane symmetry has been adopted to reduce mesh size, the magnetic vector potential being set to zero in this symmetry line, besides on the domain boundaries. The electric current density in each coil is $J = 749.219 \times 10^3$ A.m^{-2}. Fig. 3b shows results for the magnetic vector equipotentials, corresponding to the flux lines.

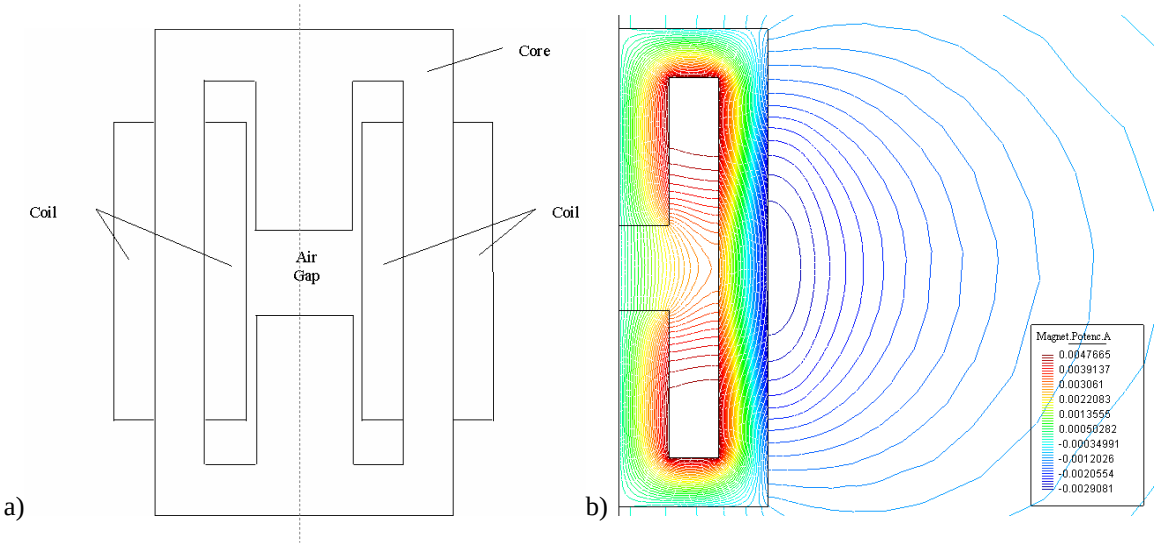

Fig. 3. a) Magnetic steering device's geometry; b) Magnetic vector equipotentials.

Experimental measurements have been performed with a gaussmeter [22] along a path ranging from the air gap's center to a point 25 mm to the side, in 5 mm steps. Table III shows a comparative analysis among our code results, FEMM's results and experimental measurements.

TABLE III. MAGNETIC DEFLECTION DEVICE – MAGNETIC INDUCTION

Pont in the path [mm]	***By* [T]: (× 10^{-4}) FEMM's results**	***Bx* [T]: (× 10^{-4}) IEN's results**	***By* [T]: (× 10^{-4}) Measurements**
0	750.7	750.7	749.1
5	748.7	748.7	745.4
10	741.4	742.2	736.2
15	727.5	730.0	718.0
20	703.8	702.3	688.7
25	668.6	684.0	653.2

B. Particle trajectory tracing

1) Trajectory in electrostatic field:

An electrostatic deflector has been simulated, consisting of two 50.0 mm length parallel plates, with a 2.0 mm gap and a potential difference of 5.0 kV applied between them.

An alfa particle has been tracked, with its mass and initial velocity corresponding to real values in the extraction region of the CV-28 Cyclotron [20]: $q = 3.20 \times 10^{-19}$ C, $m = 6.70 \times 10^{-27}$ kg and $v = 3.59 \times 10^7$ m.s^{-1}.

The domain has been bounded by the device's geometry, so as to result in an approximately uniform electric field, for comparison with the analytical result. Table IV shows the comparative analysis for vertical deflection.

TABLE IV. TRAJECTORY IN ELECTROSTATIC FIELD

Vertical deflection [mm]: Analytical result	**Vertical deflection [mm]: Numerical result**
1.1568	1.1581

Fig. 4a shows the deflector geometry, with the computed electric field, and particle's trajectory traced from left to right boundaries, while Fig. 4b shows also the finite element mesh and particle's velocity evolution. A long curvature, downwards, can be observed in both figures.

a)

Fig. 4. a) Electrostatic deflector's geometry, electric field and particle's trajectory.

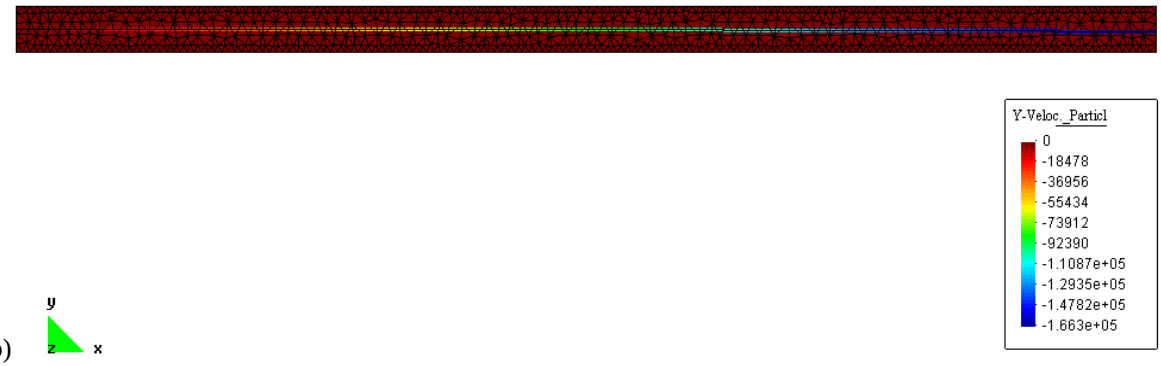

b)

Fig. 4. b) Electrostatic deflector with finite element mesh and particle's velocity evolution.

2) Trajectory in magnetostatic field:

For the magnetostatic field case, of a typical compact cyclotron has been simulated in 2D. The characteristics of this cyclotron correspond to a sector-focused – or azimuthally varying field (AVF) cyclotron –, [23], [24], and are listed in the following:

- Magnetic poles with four sectors (four hills and four valleys);
- Straight sectors (not spiraled);
- Pole diameter: 2 m;

The simulated cyclotron resembles, in a sense, some cyclotrons cited in a number of publications of stripping extraction systems, as: VINCY Cyclotron [25], DC-72 Cyclotron [13], [16], and U-400R Cyclotron [16], to cite just some references. For a first work, the simulation of this typical cyclotron

opens possibilities to simulate other cyclotrons.

Hard-edge approximation has been adopted for the magnetic induction component B_z, as can be assumed in preliminary simulations [26]. Only the last internal orbit at the extraction radius, and particle's extraction paths, are shown. Closed orbit approximation has been considered, as usually done for this type of cyclotron [27]. Closed orbit parameters have been set to:

- Azimuthally averaged magnetic induction B_{av} = 1 T;
- Average particle's radius ρ_{av} = 0.8 m;

As long as hills and valleys' angles are equal, magnetic induction on hills B_h and in valleys B_v have been set to hypothetical values around B_{av}: B_h = 1.5 T, and B_v = 0.5 T.

Results for the first simulated example is shown in the following, corresponding to a closed orbit in the cyclotron. Fig. 5a shows mesh with trajectory, while Fig. 5b shows cyclotron's geometry, magnetic induction on hills and valleys, and trajectory. Hills are shown in brown, while valleys are shown in light blue, corresponding to the magnetic induction's magnitude colors scale shown in the right side of Fig. 5b.

It is possible to notice the curvature with reduced radius on the hills, and with larger radius on the valleys, as expected.

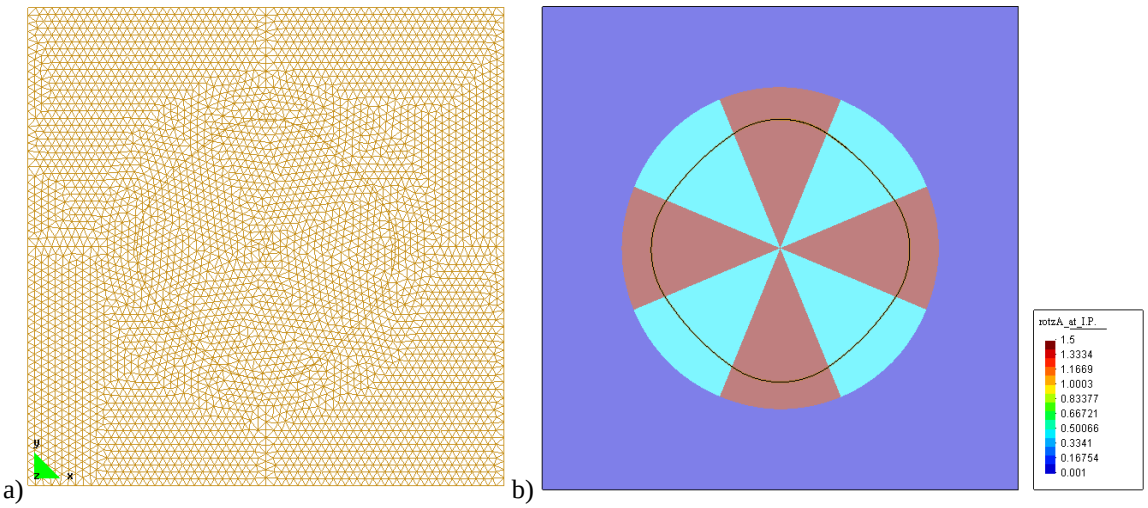

Fig. 5. a) Mesh and particle's trajectory; b) Cyclotron's geometry, magnetic induction on sectors and particle's closed orbit.

Another example has been simulated, for stripping extraction of positive ions from the cyclotron. Ratio of specific charge change has been chosen as K = 2. Fig. 6 shows the resulting trajectory.

Received 10 Aug., 2006; revised 16 Feb., 2007; accepted 27 April 2007
ISSN 1516-7399

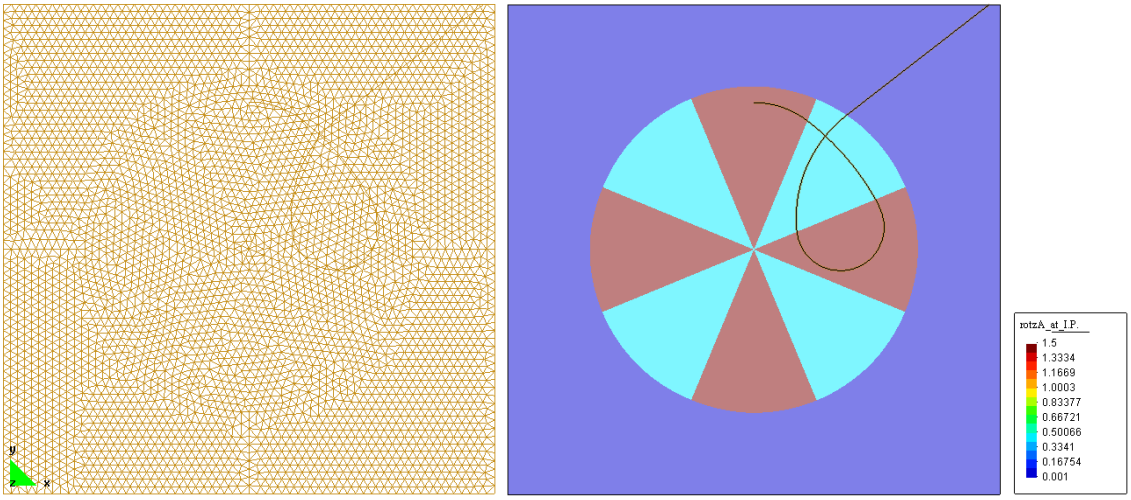

Fig. 6. a) Mesh and particle's trajectory; b) Cyclotron geometry, showing the sectors and positive ion extraction.

Strip-foil is located at angle 22.5º (see referential coordinate system in Fig. 1), what corresponds to the frontier between the right hill and the valley above it. It is possible to notice the effect of strip-foil positioning for positive ion extraction. The first part of the loop occurs within the hill, resulting in a shorter curvature radius. The second part, in turn, occurs within the valley, which causes a curvature radius enlargement and particle exit from the cyclotron.

This example has been simulated with different meshes, and the results are shown in Table V. It is possible to notice that mesh refinement improve the results, as shown by the convergence of particle's exit coordinates and velocity.

TABLE V. PARTICLE'S EXIT COORDINATES AND VELOCITY EVOLUTION WITH MESH REFINEMENT

Number of elements in the mesh	**Particle's exit coordinates [m]**	**Particle's exit velocity [m·s^{-1}]**
1926	x = 0.698	v_x = 0.711
	y = 0.715	v_y = 0.366
8004	x = 0.660	v_x = 0.692
	y = 0.750	v_y = 0.402
32454	x = 0.659	v_x = 0.691
	y = 0.752	v_y = 0.403

VI. CONCLUSIONS

The 2D magnetostatic examples show good results achieved for magnetostatic field simulations from vector potential formulation.

An alternative method for single non-relativistic particle trajectory computation in electrostatic or magnetostatic fields, has been developed and implemented. Particle trajectory tracing was achieved for both electrostatic and magnetostatic fields. In the former case, a realistic example of an electrostatic deflector was simulated, with good results, as shown in Table IV.

For the magnetostatic field case, the first cyclotron simulation shows a closed orbit at extraction radius, which agrees with theoretical predictions, with the orbit terminating over itself. Some

Received 10 Aug., 2006; revised 16 Feb., 2007; accepted 27 April 2007
ISSN 1516-7399

simulations of another example of stripping extraction of positive light ions have been performed, leading also to good results. It is clear that mesh refinement techniques improves particle trajectory computation. Thus, adaptive remeshing can be used, possibly only near particle's trajectory.

The approaches adopted for particle's trajectories computation, can be extended to 3D, by considering particle's trajectory intersection with plane equations, corresponding to the finite element faces.

Besides implementing an alternative trajectory computation method, the authors also attempt to the technique of stripping extraction of positive light ions from cyclotrons. To upgrade positive ion cyclotrons, so it achieves near 100 % extraction efficiency, one possibility is to convert it to a negative ion cyclotron. This option, though, brings several technological difficulties. Negative ion cyclotrons must have its vacuum improved, to avoid negative ion dissociation in the residual gas. Negative ion sources [28], [29], have themselves other inherent technological difficulties, specially external ones, which involve RF design, and also the challenging problem of injecting ions into cyclotron through an inflector [30]-[32].

Therefore, the stripping extraction of positive ions turns to be a very interesting alternative for positive cyclotron upgrade, if it could be tuned to accelerate light positive ions such those mentioned in this work, as: molecular Hydrogen H_2^+, Helium He^+, or other ions mentioned in the literature. A method for particle trajectory computation and tracing, such as the one presented in this work, can strongly support this kind of work.

Besides cyclotrons simulations, the design of other electromagnetic devices for accelerator or associated technologies could benefit of such a method. Examples could be accelerators of other types, beam lines and beam bending magnets, mass spectrometers, among others.

ACKNOWLEDGMENT

The authors would like to thank Prof. João P. A. Bastos, from GRUCAD/UFSC, for supplying us with his references; Dr. David Meeker, for his software FEMM, used for comparative analysis with our developed codes; and Dr. P. A. B. de Sampaio, for his suggestion on the use of the finite element identification method, described in Section III *A*. Thanks also to anyone who may have contributed with this work.

REFERENCES

[1] The Cyclotron Corporation, *Instruction and Service Manual for the Cyclotron Corporation's Model CV-28 Cyclotron - Ser. No. 238*, Jun. 1974.

[2] J. I. M. Botman, H. L. Hagedoorn; "Extraction from cyclotrons", in: S. Turner, Ed., *Proceedings of CERN Accelerator School (CAS): Cyclotrons, linacs and their applications*, 1996.

[3] C. A. F. Jorge, R. J. Jospin, J. A. D. Furlanetto, "3D electromagnetics code development based on the finite element method", in *XXVII Iberian Latin American Congress on Computational Methods in Engineering (CILAMCE 2006*), 2006, CD-ROM.

[4] C. A. F. Jorge, R. J. Jospin, J. A. D. Furlanetto, "Particle trajectory tracing and 2D electromagnetic fields simulations by finite element method", in *MOMAG 2006 - 12º SBMO - Simpósio Brasileiro de Microondas e Optoeletrônica e 7º CBMAG - Congresso Brasileiro de Eletromagnetismo*, F. Moreira, R. C. Mesquita, Eds. 2006, CD-ROM.

Received 10 Aug., 2006; revised 16 Feb., 2007; accepted 27 April 2007
ISSN 1516-7399

[5] C. A. F. Jorge, R. J. Jospin, D. E. S. Nery, "Simulation of electromagnetic fields through finite element method with adaptive remeshing", in *XXV Iberian Latin American Congress on Computational Methods in Engineering (CILAMCE 2004*), P. R. M. Lyra, *et al.*, Eds. 2004, CD-ROM.
[6] C. K. Birdsall, A. B. Langdon, *Plasma Physics via Computer Simulations*, New York: McGraw-Hill, 1985.
[7] T. Tajima, *Computational Plasma Physics: With Applications to Fusion & Astrophysics*, Boston, MA: Addison-Wesley, 1988.
[8] Y. C. Polli; *Cálculos de Trajetórias de Elétrons em Estruturas Magnéticas*, Tese de Mestrado, Universidade de São Paulo, 1999.
[9] M. Gyimesi, V. Zhulin, D. Ostergaard, "Particle trajectory tracing in ANSYS". *Nuclear Instruments and Methods in Physics Research A*, vol. 427, n. 1-2, pp. 408-411, 1999.
[10] G. Dhatt, G. Touzot, *Une Présentation de la Méthode des Éléments Finis*, Paris: Maloine S. A. Éditeur, 1981.
[11] S. J. Salon, *Finite Element Analysis of Electrical Machines*, Boston, MA: Kluwer Academic Publishers, 1995.
[12] J. Peraire, M. Vahdati, K. Morgan, O. C. Zienkiewicz, "Adaptive remeshing for compressible flow computation", *J. Comput. Phys.*, n. 72, pp. 449-466, 1987.
[13] D. Solivajs, *et al.*; "A study of charge-exchange beam extraction from the multi-purpose isochronous cyclotron DC-72", *Journal of Electrical Engineering*, vol. 55, n. 7-8, pp. 201-206, 2004.
[14] J. L. Ristic-Djurovic; "Stripping extraction of positive ions from a cyclotron", *Physical Review Special Topics – Accelerators and Beams*, vol. 4, n. 12, Dec. 2001.
[15] J. L. Ristic-Djurovic, S. Cirkovic; "Unidirectional stripping extraction from a cyclotron which accelerates light as well as heavy ions", *Physical Review Special Topics – Accelerators and Beams*, vol. 6, March 2003.
[16] O. N. Borisov, G. G. Gulbekian, D. Solivajs; "Numerical simulation of beam extraction from DC-72 and U-400R Cyclotron by stripping", *Proceedings of the XIX Russian Particle Accelerator Conference (RuPAC 2004)*, pp. 180-182, 2004.
[17] E. Baron, B. Delaunay; "Stripping of high-energy krypton ions by various solid materials", *Physics Review A*, vol. 12, n. 1, pp. 40-44, July 1975.
[18] K. Shima, T. Ishihara, T. Mikumo; "Empirical formula for the average equilibrium charge-state of heavy ions behind various foils", *Nuclear Instruments and Methods in Physics Research*, vol. 200, pp. 605-608, 1982.
[19] J. P. A. Bastos, *Eletromagnetismo para Engenharia: Estática e Quase-Estática*, Florianópolis: Editora da UFSC, 2004.
[20] J. A. D. Furlanetto, *Projeto e Desenvolvimento de um Varredor de Feixe para Utilização em Aceleradores de Partículas Carregadas*, Tese de Mestrado, Instituto Militar de Engenharia, 1998.
[21] D. Meeker, *Finite Element Method Magnetics, Version 4.0, User's Manual*, Jan. 2006.
[22] Gaussmeter model GM1A manual, Applied Magnetics Laboratory, Inc.
[23] J. D. Livingood; *Principles of Cyclic Particle Accelerators*, Argonne National Laboratories, 1960.
[24] M. S. Livingston, J. P. Blewett; *Particle Accelerators*, New York: McGraw-Hill Book Company, 1962.
[25] O. N. Borisov, J. L. Ristic-Djurovic; "Beam extraction systems of the VINCY Cyclotron", *Proceedings of the Fifth European Particle Accelerator Conference (EPAC'96)*, pp. 2432-2434, 1996.
[26] M. Yoon, J. S. Chai, J. W. Kim, W. Y. Yang, S. Oh; "Initial design of a 13 MeV cyclotron for positron emission tomography ", in *Proceedings of the First Asian Particle Accelerator Conference (APAC'98)*, pp. 798-800, 1998.
[27] T. Stammbach; "Introduction to cyclotrons", in: S. Turner, Ed., *Proceedings of CERN Accelerator School (CAS): Cyclotrons, linacs and their applications*, 1996.
[28] C. E. Hill; "Ion and electron sources", in: S. Turner, Ed., *Proceedings of CERN Accelerator School (CAS): Cyclotrons, linacs and their applications*, 1996.
[29] D. P. Moehs, J. Peters, J. Sherman; "Negative hydrogen ion sources for accelerators", *IEEE Transactions on Plasma Science*, vol. 33, n. 6, pp. 1786-1798, 2005.
[30] P. Mandrillon; "Injection into cyclotrons", in: S. Turner, Ed., *Proceedings of CERN Accelerator School (CAS): Cyclotrons, linacs and their applications*, 1996.
[31] B. F. Milton, J. B. Pearson; "CASINO User's Guide and Reference Manual", *Design Note TRI-DN-89-19*, TRIUMF, 1989.
[32] L. Milinkovic; "RELAX3D Spiral Inflectors", *Design Note TRI-DN-89-21*, TRIUMF, 1992.

Brazilian Microwave and Optoelectronics Society-SBMO *Received 10 Aug., 2006; revised 16 Feb., 2007; accepted 27 April 2007*
ISSN 1516-7399